

Single-Molecule Study of the Inhibition of HIV-1 Transactivation Response Region DNA/DNA Annealing by Argininamide

Christy F. Landes,^{†,§} Yining Zeng,[†] Hsiao-Wei Liu,[†] Karin Musier-Forsyth,[‡] and Paul F. Barbara^{*,†}

Contribution from the Department of Chemistry and Biochemistry, Center for Nano and Molecular Science and Technology, The University of Texas at Austin, Austin, Texas 78712, and Department of Chemistry, The Ohio State University, Columbus, Ohio 43210

Received March 2, 2007; E-mail: p.barbara@mail.utexas.edu

Abstract: Single-molecule spectroscopy was used to examine how a model inhibitor of HIV-1, argininamide, modulates the nucleic acid chaperone activity of the nucleocapsid protein (NC) in the minus-strand transfer step of HIV-1 reverse transcription, in vitro. In minus-strand transfer, the transactivation response region (TAR) RNA of the genome is annealed to the complementary "TAR DNA" generated during minus-strand strong-stop DNA synthesis. Argininamide and its analogs are known to bind to the hairpin bulge region of TAR RNA as well as to various DNA loop structures, but its ability to inhibit the strand transfer process has only been implied. Here, we explore how argininamide modulates the annealing kinetics and secondary structure of TAR DNA. The studies reveal that the argininamide inhibitory mechanism involves a shift of the secondary structure of TAR, away from the NC-induced "Y" form, an intermediate in reverse transcription, and toward the free closed or "C" form. In addition, more potent inhibition of the loop-mediated annealing pathway than stem-mediated annealing is observed. Taken together, these data suggest a molecular mechanism wherein argininamide inhibits NC-facilitated TAR RNA/DNA annealing in vitro by interfering with the formation of key annealing intermediates.

Introduction

In the minus-strand transfer of HIV-1 reverse transcription, the transactivation response region (TAR) RNA of the genome is annealed to the complementary "TAR DNA" in minus-strand strong-stop DNA via a multistep process that is chaperoned by the nucleocapsid protein (NC). A molecular-level understanding of the minus-strand transfer process of HIV-1 has emerged in recent years.^{1–10} Several mechanistic insights into these processes have been obtained by applying single-molecule

spectroscopy (SMS) to an in vitro model for minus-strand transfer, which is portrayed in Figure 1.^{4–6,11} This model involves annealing of a TAR DNA hairpin to a complementary TAR RNA hairpin, mimicking a key step in reverse transcription.^{2,12,13}

Fluorescence resonance energy transfer SMS (SMFRET) has been extensively used to study two main aspects of annealing: (i) the kinetics of annealing under various conditions and (ii) the secondary structure of nucleic acid intermediates in the annealing mechanism. In the recently proposed mechanism for the annealing of complementary TAR hairpins (eqs i–iii in Figure 1), the chaperone function of NC arises from two processes. First, NC partially melts the closed "C" secondary structure of TAR hairpins producing a partially open "Y" structure containing single-stranded regions that promote the nucleation of annealing.^{11,14} In the presence of NC (and low Mg²⁺ concentration), "Y" is more stable than "C", due to preferential interaction of NC with the single-strand regions of "Y". Second, NC increases the rate of the nucleation of annealing by weakly associating the two reacting hairpins in an encounter complex.^{4,6}

[†] The University of Texas at Austin.

[‡] The Ohio State University.

[§] Present address: Department of Chemistry, University of Houston, Houston TX 77204-5003.

- (1) Hong, M. K.; Harbron, E. J.; O'Connor, D. B.; Guo, J.; Barbara, P. F.; Levin, J. G.; Musier-Forsyth, K. *J. Mol. Biol.* **2003**, *325*, 1.
- (2) Bernacchi, S.; Stoylov, S.; Piémont, E.; Ficheux, D.; Roques, B. P.; Darlix, J. L.; Mély, Y. *J. Mol. Biol.* **2002**, *317*, 385.
- (3) Beltz, H.; Azoulay, J.; Bernacchi, S.; Clamme, J. P.; Ficheux, D.; Roques, B.; Darlix, J. L.; Mély, Y. *J. Mol. Biol.* **2003**, *328*, 95.
- (4) Liu, H. W.; Cosa, G.; Landes, C. F.; Zeng, Y.; Kovaleski, B. J.; Mullen, D. G.; Barany, G.; Musier-Forsyth, K.; Barbara, P. F. *Biophys. J.* **2005**, *89*, 3470.
- (5) Zeng, Y.; Liu, H. W.; Landes, C. F.; Kim, Y. J.; Ma, X.; Zhu, Y.; Musier-Forsyth, K.; Barbara, P. F. *Proc. Natl. Acad. Sci. U.S.A.*, in press.
- (6) Liu, H. W.; Zeng, Y.; Landes, C. F.; Kim, Y. J.; Zhu, Y.; Ma, X.; Vo, M.; Musier-Forsyth, K.; Barbara, P. F. *Proc. Natl. Acad. Sci. U.S.A.* **2007**, *104*, 5261.
- (7) Guo, J.; Wu, T.; Anderson, J.; Kane, B. F.; Johnson, D. G.; Gorelick, R. J.; Henderson, L. E.; Levin, J. G. *J. Virol.* **2000**, *74*, 8980.
- (8) Guo, J.; Wu, T.; Kane, B. F.; Johnson, D. G.; Henderson, L. E.; Gorelick, R. J.; Levin, J. G. *J. Virol.* **2002**, *76*, 4370.
- (9) Heilman-Miller, S. L.; Wu, T.; Levin, J. G. *J. Biol. Chem.* **2004**, *279*, 44154.
- (10) Levin, J. G.; Guo, J.; Rouzina, I.; Musier-Forsyth, K. *Prog. Nucleic Acid Res. Mol. Biol.* **2005**, *80*, 217.

- (11) Cosa, G.; Harbron, E. J.; Zeng, Y.; Liu, H. W.; O'Connor, D. B.; Eta-Hosokawa, C.; Musier-Forsyth, K.; Barbara, P. F. *Biophys. J.* **2004**, *87*, 2759.
- (12) You, J. C.; McHenry, C. S. *J. Biol. Chem.* **1994**, *269*, 31491.
- (13) Driscoll, M. D.; Hughes, S. H. *J. Virol.* **2000**, *74*, 8785.
- (14) Cosa, G.; Zeng, Y.; Liu, H. W.; Landes, C. F.; Makarov, D. E.; Musier-Forsyth, K.; Barbara, P. F. *J. Phys. Chem. B* **2006**, *110*, 2419.

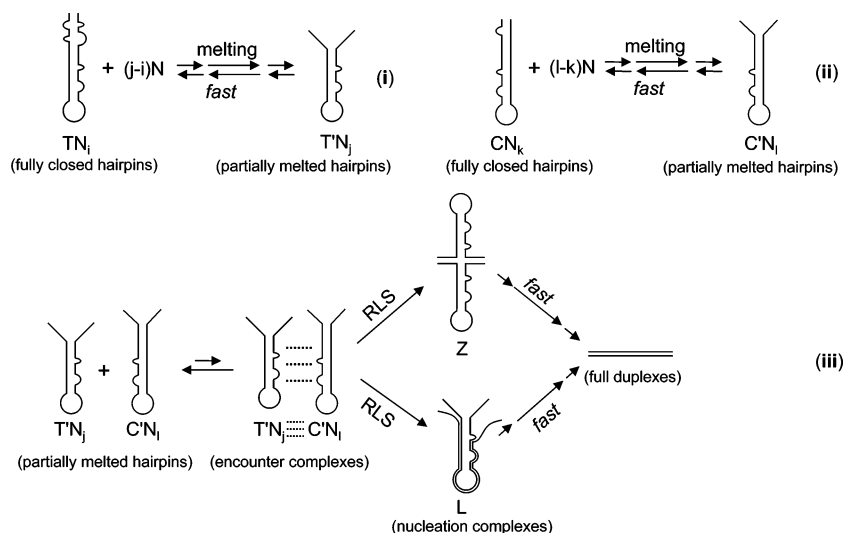


Figure 1. Hypothetical kinetic scheme of TAR DNA annealing to its complement chaperoned by HIV-1 NC. Here, T denotes TAR DNA, and C denotes complementary cTAR DNA or TAR RNA. The term N denotes the nucleocapsid protein, NC. In this scheme, N bound to T and C leads to a partially melted structure, namely, the “Y” form of T (T′) and C (C′). The subscripts i, j, k, and l are used to describe the number of NCs bound to nucleotides. Two partially melted hairpins form an encounter complex that leads to the formation of nucleation complexes. The annealing can go through either zipper nucleation or loop nucleation, thereby forming zipper nucleation complexes (Z) or loop nucleation complexes (L) that lead to the formation of fully annealed duplexes.

The major focus of this paper is the development of a molecular-level understanding of the mode of action of model nucleic acid binding molecules, such as arginine and arginamide, for inhibiting annealing processes, especially minus-strand transfer. Both molecules have been shown to exhibit specific binding affinity for the uracil bulge region in the TAR RNA hairpin.^{15–18} The binding specificity between TAR RNA and the argininamide analogs is of interest because of the role that Tat, HIV’s transcriptional transactivator, plays in binding to TAR RNA through its arginine residues at crucial steps during the viral life cycle.^{19,20} It has been proposed that the next generation of inhibitors may be developed from compounds that can bind TAR RNA similarly to the active native structure and induce structural conformations that inhibit functionality.²¹ Such inhibition may involve a decrease in hairpin flexibility that is associated with argininamide binding.²² To date, studies have demonstrated conclusively that argininamide binds to TAR RNA,^{15–18} to TAR RNA/DNA composites,²³ and to various other DNA loop structures.^{24,25} Thus, it is important to obtain a clearer understanding of the role such inhibitors may play in the overall process of minus-strand transfer. No detailed analysis has been performed on either argininamide’s specificity for the complementary TAR DNA hairpin nor its efficiency at inhibiting minus-strand transfer. Such analyses, of even model binding agents, are important to the development of effective inhibitors.

Herein we use SMFRET to study how argininamide, as compared to the “simple” divalent cation Mg^{2+} , modulates the chaperone activity of NC by examining its effect on the annealing kinetics of TAR DNA with complementary oligonucleotides, *in vitro*. Our goal is to obtain detailed information on the molecular scale action of HIV-1 inhibitors for minus-strand transfer, which could aid in the development of better inhibitors. The single-molecule studies reveal that argininamide measurably suppresses the NC-induced partial melting of TAR. Previous studies with short targeted oligonucleotides suggest that annealing can be nucleated in either the hairpin loop region of TAR, producing a so-called loop “L” nucleation complex, or in the terminal region of TAR, producing a so-called zipper “Z” nucleation complex.^{4,5} It is appropriate to use DNA analogs for these types of reactions because we have recently offered evidence that the reaction results are consistent with the DNA–RNA annealing reactions associated with minus-strand transfer.^{5,6} By using short, targeted oligonucleotides we examine the effects of argininamide on each of these two previously identified sites for the nucleation of annealing. Argininamide is reported herein to inhibit NC-chaperoned zipper- and loop-type annealing with higher inhibition of the latter. The effects of argininamide on annealing are compared to the effects of varying concentrations of Mg^{2+} , which also is found to exhibit pathway-specific inhibition.

Experimental Section

Sample Preparation. Purified DNA sequences (see Figure 2) containing the appropriate functionalization (i.e., biotin for hairpin immobilization and donor (Cy3) and acceptor dye (Cy5)) were acquired from TriLink Biotechnologies (San Diego, CA). The HIV-1 NC protein for these experiments was prepared by solid-phase synthesis or by *E. coli* expression, both described previously.^{4,11} All reagents were molecular biology and/or HPLC grade.

Clean coverslips were treated with Vectabond/acetone 1% w/v solutions (Vector Laboratories, Burlingame, CA) for 5 min. The coverslips were then rinsed with H_2O and dried under N_2 . Each coverslip was pegylated and biotinylated, after which a reaction chamber with

- (15) Tan, R.; Frankel, A. D. *Biochemistry* **1992**, *31*, 10288.
 (16) Puglisi, J. D.; Tan, R.; Calnan, B. J.; Frankel, A. D.; Williamson, J. R. *Science* **1992**, *257*, 76.
 (17) Pitt, S. W.; Majumdar, A.; Serganov, A.; Patel, D. J.; Al-Hashimi, H. M. *J. Mol. Biol.* **2004**, *338*, 7.
 (18) Dayie, K. T.; Brodsky, A. S.; Williamson, J. R. *J. Mol. Biol.* **2002**, *317*, 263.
 (19) Berkhout, B.; Silverman, R. H.; Jeang, K. T. *Cell* **1989**, *59*, 273.
 (20) Brigati, C.; Giacca, M.; Noonan, D. M.; Albin, A. *FEMS Microbiol. Lett.* **2003**, *220*, 57.
 (21) Davis, B.; Afshar, M.; Varani, G.; Murchie, A. I. H.; Karn, J.; Lentzen, G.; Drysdale, M.; Bower, J.; Potter, A. J.; Starkey, I. A.; Swarbrick, T.; Aboul-ela, F. *J. Mol. Biol.* **2004**, *336*, 343.
 (22) Tinoco, I., Jr.; Collin, D.; Li, P. T. X. *Biochem. Soc. Trans.* **2004**, *32*, 757.
 (23) Landt, S. G.; Tipton, A. R.; Frankel, A. D. *Biochemistry* **2005**, *44*, 6547.
 (24) Robertson, S. A.; Harada, K.; Frankel, A. D. *Biochemistry* **2000**, *39*, 946.
 (25) Lin, C. H.; Wang, W.; Jones, R. A.; Patel, D. J. *Chem. Biol.* **1998**, *5*, 555.

Oligonucleotide	Primary Structure	
D/A-TAR DNA	5'-Cy3- TGGGTTCCCTAGTTAGCCAGAGAGCTCT(biotin)C AGGCTCAGATCTGGTCTAACCAGAGAGACCCTT TT-Cy5-3'	<p>The diagram shows a DNA hairpin structure with 5' and 3' ends. The top part is labeled 'Zipper Region' and the bottom part is labeled 'Loop Region'. Shaded boxes highlight complementary regions for the four oligonucleotides listed in the table.</p>
D-TAR DNA	5'-Cy3- TGGGTTCCCTAGTTAGCCAGAGAGCTCT(biotin)C AGGCTCAGATCTGGTCTAACCAGAGAGACCCTT TT-3'	
inverted D-TAR DNA	5'-Cy3- TGGGTTCCCTAGTTAGCCAGAGAGCTCTCAGGCT CAGATCTGGTCTAACCAGAGAGACCCTTTT(biotin))-3'	
A-zipper mimic, Z	5'-GGGTCTCTCTGGCTAGGGAACCCTTTT-Cy5-3'	
A-loop mimic, L	5'-AGATCTGAGCCTGAGAGCTCTCTT-Cy5-3'	

Figure 2. (Left) Primary sequences of the DNA oligonucleotides used in the present work are listed, along with the Cy3/Cy5 and biotin functionalization of each species. (Right) The predicted secondary structure of TAR DNA along with the regions of complementarity for each of the oligonucleotides (shaded regions) are illustrated.

inlet and outlet ports (Nanoport, Upchurch Scientific, Oak Harbor, WA) was glued on top. The chambers were rinsed with distilled deionized water (50 μ L) following each incubation step. The details of this process are described in earlier work.⁴

Each chamber was treated with streptavidin (Molecular Probes, Eugene, OR; 0.2 mg/mL in 25 mM HEPES buffer) and subsequently with the appropriately labeled biotinylated TAR DNA. Standard D-TAR DNA and inverted D-TAR DNA were used interchangeably, depending on the type of reaction being performed. Past experiments have demonstrated a small (but measurable) effect of loop annealing rates depending on the biotin location in the loop region.⁴ Reactant solutions, which were delivered by syringe pumps,^{4,11} contained HEPES buffer (25 mM), MgCl₂ (various concentrations as noted in the text), NaCl (40 mM), and an oxygen scavenger system (2-mercaptoethanol 1% v/v, β -D(+)-glucose 3% w/v (Sigma-Aldrich, St. Louis, MO), glucose oxidase 0.1 mg/mL and catalase 0.02 mg/mL (all Roche Applied Science, Hague Road, IN)).^{26,27} Additional reactants were 400 nM NC and L-argininamide \cdot 2HCl (Sigma-Aldrich, St. Louis, MO) in the buffered reactant solution described above. The Na⁺ concentration for all reactions was 40 mM. The Mg²⁺ concentration was varied for each experiment, and the relevant concentrations are noted in the figure captions.

Data Collection. The home-built sample scanning confocal optical/data collection system used in these measurements is based on a Zeiss inverted microscope.¹¹ The sample flow-cell is scanned by a Queensgate X,Y scanning stage (NPW-XY-100A, Queensgate, Torquay, U.K.). A high numerical aperture, oil immersion microscope objective (Zeiss Fluor, 100 \times , NA 1.3) was used to focus the excitation light (514 nm) and collect the emission. The donor and acceptor fluorescence were separated by a dichroic beam splitter (Chroma 630 DCXR, Chroma Tech., VT) into two beams, and each was detected by an avalanche photodiode (APD) (Perkin-Elmer Optoelectronics SPCM-AQR-15, Vaudreuil, QC, Canada).

Two modes were used to collect SMFRET data in this paper, the *confocal kinetic mode* and the *individual trajectory mode*. In the *confocal kinetic mode*, scanning confocal donor and acceptor images were acquired at several times, t , during the course of annealing reactions.⁴ The annealing reactions were initiated by beginning the flow of a freshly prepared solution of NC plus either Z or L oligonucleotides into the flowing sample cell, which already contained a coverslip coated

with immobilized TAR hairpins. In the argininamide reactions, argininamide was preincubated with the appropriate buffer/salt solution and/or the appropriate complementary DNA sequence and flowed into the reaction chamber for measurement. Donor and acceptor emission intensities were calculated from the individual fluorescence spots (due to individual immobilized dye-labeled hairpins) in the confocal images at various elapsed times, t , from the initiation of the Z or L oligonucleotide flow. The time spacing between images was typically hundreds of seconds for longer reactions but was reduced to 25 s for increased resolution in faster reactions. In-house software was written to find molecules, correct for drift, photobleaching, blinking, and crosstalk, and calculate SMFRET efficiency, as described below, for each molecule.

In the *individual trajectory mode*, the microscope was positioned to focus on an individual immobilized hairpin, and time, t , trajectories of donor and acceptor emission intensities were recorded with 1 ms time resolution for several seconds. The procedure was repeated for hundreds of molecules for each sample.

For both *individual trajectory mode* and *kinetic mode*, the corrected donor and acceptor intensities, $I_D(t)$ and $I_A(t)$, respectively, were used to calculate directly the time trajectory of the apparent FRET efficiency, $E_A(t)$, as in

$$E_A(t) = \frac{I_A(t)}{I_A(t) + I_D(t)} \quad (1)$$

$E_A(t)$ is related to the actual FRET efficiency, $E_{\text{FRET}}(t)$, by the inclusion of the dye quantum efficiencies, ϕ_i , and detector quantum efficiencies, η_i , as in

$$E_{\text{FRET}}(t) = \frac{I_A(t)}{I_A(t) + I_D(t) \frac{\phi_A \eta_A}{\phi_D \eta_D}} \quad (2)$$

In the case of the current experimental setup, it was determined that $E_A(t) \sim E_{\text{FRET}}(t)$. The collected donor and acceptor signals were corrected for background emission/noise and donor/acceptor crosstalk due to overlapping emission as previously described.¹¹

For the *individual trajectory mode* only, single-molecule cross-correlations of $I_D(t)$ versus $I_A(t)$ were calculated by eq 3.

$$C(\tau) = \frac{\langle \delta I_D(t) \delta I_A(t + \tau) \rangle}{\langle I_D \rangle \langle I_A \rangle} = \frac{\langle I_D(t) I_A(t + \tau) \rangle}{\langle I_D \rangle \langle I_A \rangle} - 1 \quad (3)$$

(26) Ha, T. *Curr. Opin. Struct. Biol.* **2001**, *11*, 287.

(27) Harada, Y.; Sakurada, K.; Aoki, T.; Thomas, D. D.; Yanagida, T. *J. Mol. Biol.* **1990**, *216*, 49.

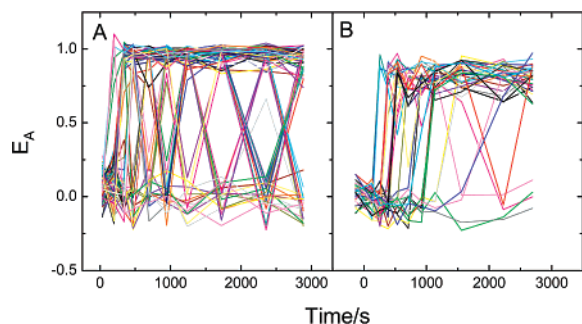


Figure 3. Single-molecule E_A trajectories of ~ 100 molecules during the annealing of (A) 10 nM A-zipper DNA or (B) 10 nM A-loop DNA to immobilized D-TAR at 1 mM Mg^{2+} and 440 nM NC, collected by the confocal kinetic mode.

E_A autocorrelation analysis was acquired using the single-molecule cross-correlation curves according to eq 4, as described in detail in a previous study.¹¹ The measured autocorrelation amplitude will be referred to as E_{AAC} .

$$E_A \text{ autocorrelation}(\tau) = C(\tau) \left(-\frac{\langle I_D \rangle}{\langle I_A \rangle} \right) \quad (4)$$

Results and Discussion

Basic Annealing Kinetics. The kinetics of NC-induced annealing of donor-labeled TAR hairpins (D-TAR) with each complementary DNA oligonucleotide, i.e., A-zipper mimic (Z) and A-loop mimic (L), were investigated by time-resolved SMFRET. The primary structures of the various oligonucleotides are shown in Figure 2. The “D” or “A” preceding each sequence term implies a donor or an acceptor dye, respectively. SMFRET time trajectories for ~ 100 single TAR DNA hairpins annealing with each oligonucleotide (in the absence or presence of argininamide) can be measured by the confocal kinetic mode, as described in the data collection section, above. Examples of both Z and L annealing (in the absence of argininamide) are shown in Figure 3, parts A and B, respectively. By examining the time trajectories for each type of reaction, one can obtain a statistical distribution of reaction times (observed in Figure 3A as a distribution of on times required for different molecules to switch from reactant, with $E_A \sim 0$, to product, with $E_A \sim 0.96$, for the D-TAR/Z complex) that yield an experimentally determined rate constant. One can also observe directly the equilibrium process for each two-state reaction (as exhibited by discrete jumps between the reactant unannealed hairpin, with $E_A \sim 0$, and an annealed D-TAR/Z complex, with $E_A \sim 0.96$).⁴ Analogous two-state annealing was observed for D-TAR/L annealing (Figure 3B), although the annealed form in this case has a lower FRET value ($E_A \sim 0.8$) due to a longer D/A distance. Although the temporal resolution in the confocal kinetic mode is lower than with the individual trajectory mode, by comparing the two types of annealing in this way we can observe a statistically significant number of molecules and simultaneously confirm that, indeed, Z-type annealing is both faster and more reversible than L-type annealing. For the faster Z-type annealing, collection times were decreased to improve temporal resolution.

The two-state nature of the annealing process is especially apparent by analyzing an ensemble of SMFRET trajectories in the form of SMFRET histograms, as shown in Figure 4A–C

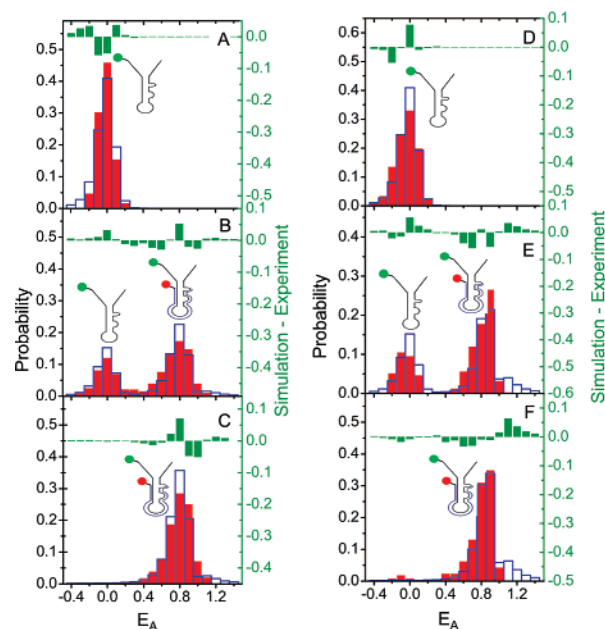


Figure 4. (Left) Experimental (red) and simulated (blue) SMFRET histograms for the reaction of immobilized D-TAR molecules with A-loop mimic (10 nM) at 1 mM Mg^{2+} (red) in the absence (A–C) and presence (D–F) of 2 mM argininamide at $t = 0$ (A and C), $t = \tau$ (B and E), and $t = \infty$ (C and F). The difference between the simulated and experimental histograms is shown in green.

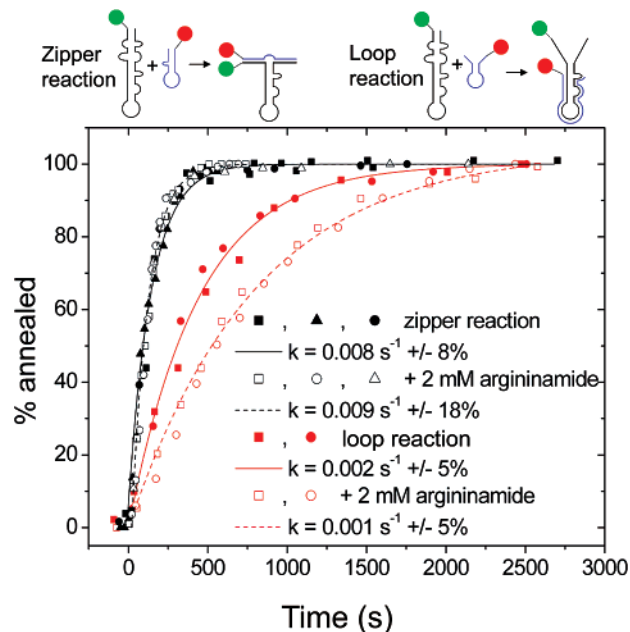


Figure 5. Effects of argininamide (2 mM) on NC-chaperoned loop-type (red) and zipper-type (black) annealing kinetics (with 10 nM of each oligomer in solution) are compared in the presence of 1 mM Mg^{2+} and 400 nM NC. The curves associated with each type of reaction correspond to a single-exponential fit with the rates indicated in the inset. The fits were achieved using three separate experimental time trajectories for each zipper reaction and two separate experimental trajectories for each loop reaction, as indicated by the different data symbols in the figure. The data/curves have been normalized, for presentation.

for D-TAR molecules annealing to L at various reaction times in the absence of argininamide. These data clearly show two distinct peaks, which are assigned to the unannealed and annealed forms (see the schematic structures at the top of Figure 4). There is excellent agreement between the observed histo-

grams and simulated histograms (blue curves) generated from a two-state, irreversible, first-order model at $t = 0$, $t = \tau$, and $t = \infty$ (Figure 4, parts A, B, and C, respectively). The small residual differences (green) between each simulated histogram and the corresponding experimental set are likely due to slight imperfections in the model, which is described in detail in the Supporting Information. This type of comparison is especially important at intermediate reaction times, such as a $t \sim \tau$, where subtle deviations from two-state behavior might be expected in the experimental system. Deviation from two-state behavior is, however, observed neither for TAR DNA/L annealing, nor for the similar reaction in the presence of argininamide (Figure 4D–F), nor for TAR DNA/Z annealing (data not shown) in the presence or absence of argininamide.

The dynamics of L- and Z-type annealing have been shown to depend on many factors such as oligomer concentration, NC concentration, and the ionic strength of Mg^{2+} and, to a lower extent, Na^+ .^{4,11,14} The complex role of Mg^{2+} will be discussed in more detail below, but one can examine the role of argininamide in pseudo-first-order conditions by maintaining a constant, high concentration of all species relative to the immobilized TAR DNA hairpin and varying only the argininamide concentration. Figure 5 shows that the observed annealing kinetics are well-fit by a simple first-order treatment. The percent reaction in the figure has been calculated directly from $E_A(t)$ data using a E_A threshold of 0.4 to distinguish annealed and unannealed hairpins. The observed simple first-order behavior is, furthermore, consistent with a pseudo-first-order kinetic scheme



resulting from the large excess concentration of Z or L hairpins and the high NC concentration, which ensures saturated NC binding. The annealing kinetics are approximately irreversible, under the relatively high Mg^{2+} concentration used in this study, but are reversible at lower Mg^{2+} concentration, as described earlier.⁴ As previously demonstrated,⁴ the NC-chaperoned loop-type annealing occurs at a slower rate than zipper-type annealing.

As summarized in Figure 5, the data from 10 separate experiments show that the Z-type annealing rate is unaffected, whereas the L-type reaction rate is decreased by 50%, in the presence of 2 mM argininamide. It is important to note that, in this example, the argininamide is present at twice the Mg^{2+} concentration, which is in itself high enough to influence strongly the equilibrium stability of the double-stranded DNA products or reactants (see ref 14 for a detailed discussion). Each reactant oligomer is present in nanomolar amounts, and the immobilized TAR DNA concentration is immeasurably lower. Table 1 compares second-order rate constants for Z and L annealing reactions at several different argininamide concentrations, including a limiting case performed at 10 mM that will be discussed below. Additional data from experiments performed at 0.2 mM argininamide (at which concentration Mg^{2+} has been shown to affect the annealing dynamics) are not included because they are indistinguishable from the control. The results can be summarized as follows: it is possible to observe specificity of argininamide in inhibiting L-type annealing, as highlighted by the 2 mM data; at very high concentrations both

Table 1. Apparent Second-Order Rate Constant k_a for the NC-Chaperoned Annealing of TAR DNA to Its Zipper/Loop Complementary Oligomers at Various Argininamide Concentrations^a

[Arg] (10^{-3} M)	zipper ($10^5 \text{ s}^{-1} \text{ M}^{-1}$)	loop ($10^5 \text{ s}^{-1} \text{ M}^{-1}$)
0	8 ± 1^b	2.0 ± 0.1^b
1	7^c	2^c
2	9 ± 2^b	1.00 ± 0.05^b
10	0.03^d	0.002^d

^a The NC and Mg^{2+} concentrations were 400 nM and 1 mM, respectively. ^b Values were determined from the single-molecule kinetic measurements shown in Figure 5. ^c Error was not estimated. ^d Due to the increasing impact of artifacts, such as photobleaching, on single-molecule counting when the rate is slow, especially at high argininamide concentration, these values were estimated from the pseudo-first-order rate equation $\ln R/R_0 = -kt$. The ratio of the number of unreacted molecules (R) after time t to the number of molecules before reaction started (R_0) was determined from the ratio of two peak areas in the E_A histogram shown in Figure 6, and it was calculated to be 0.726 for zipper annealing and 0.976 for loop annealing. The t was roughly estimated to be 3 h.

pathways are inhibited, most likely due to high ionic strength; and meaningful inhibition of either reaction, regardless of its molecular origin, can only be achieved at a prohibitively (and toxically) high argininamide concentration. These results can be contrasted with the Mg^{2+} dependence of each pathway. The kinetic curves shown in Figure 5 were obtained at 1 mM Mg^{2+} . When the reactions are performed at 2 mM Mg^{2+} ,⁴ both zipper and loop annealing rates decrease, with a more dramatic effect observed for the loop rate. Additional data on this topic is included in the Supporting Information.

Loop versus Zipper Annealing. We have observed that argininamide can inhibit the rate of NC-chaperoned annealing. The inhibitory effect of argininamide is, however, greater for loop-type annealing than for zipper-type annealing, see Figure 5 and Table 1. For argininamide concentrations higher than 2 mM, the annealing rates were too slow to measure accurately by direct kinetic measurements of the type in Figure 5 due to dye photobleaching and sample drift. Fortunately, the rates of the zipper versus loop modes could be estimated from single time-point (extent of reaction) determinations (assuming first-order kinetics) using the relative concentration of annealed and unannealed hairpins at a chosen time after initiating the reaction. The relative concentrations were determined from E_A histograms of the type shown in Figure 6, which were calculated from a set of E_A trajectories, recorded in *individual trajectory mode*, in a short time interval (~ 30 min) after the annealing reaction was initiated.

At negative times, i.e., before the nonimmobilized hairpin was flowed into the sample cell, the E_A histogram only exhibited a single peak, i.e., due to unannealed D-TAR, with $E_A \sim 0$ (Figure 6A). Figure 6B portrays a histogram calculated from trajectories that were recorded 30 min after the initiation of D-TAR annealing with the loop oligonucleotide. The two peaks in the histogram are assigned to the TAR/loop annealed product ($E_A \sim 0.8$) and the unreacted D-TAR ($E_A \sim 0$) hairpins, resulting from the slow annealing kinetics. The E_A histogram for the analogous reaction with the A-zipper mimic collected after ~ 30 min reveals 100% formation of the TAR/zipper annealed product, due to the faster annealing rate for this type of nucleation (Figure 6E).

As mentioned above, the inhibition of annealing is considerably more effective for loop-type annealing (Figure 6D) than

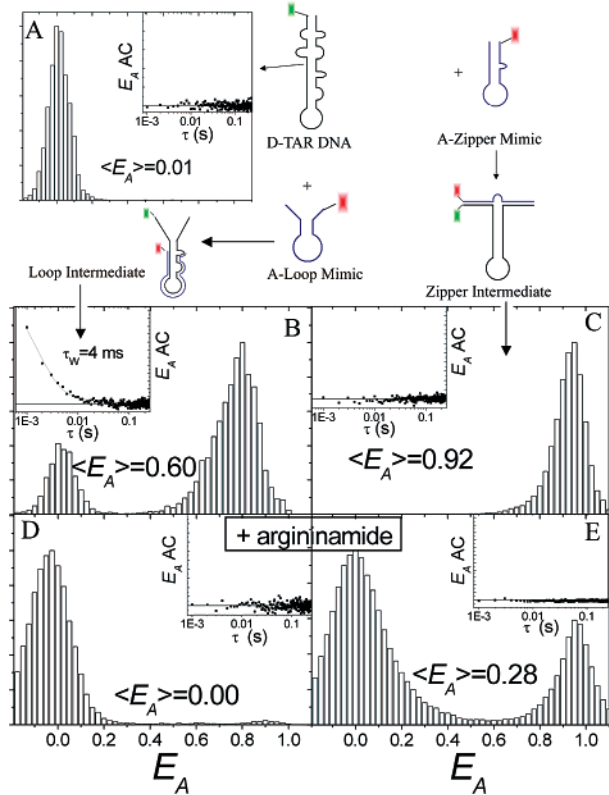


Figure 6. (A) Ensemble E_A histogram for D-TAR DNA is shown. (B and C) The ensemble E_A histograms of the loop (B) and zipper (C) reactions alone and in the presence of 10 mM argininamide (D and E) are presented with the respective E_A autocorrelations (insets).

zipper-type annealing (Figure 6C). The loop annealing rate is reduced by a factor of 1000 by 10 mM argininamide, whereas the zipper annealing rate is only reduced by a factor of ~ 300 at this saturating argininamide condition (Table 1). This effect is even more apparent at 2 mM argininamide, where the zipper annealing rates are not significantly different from the argininamide free results, but the loop annealing rate is reduced 2-fold in its presence. Further evidence that argininamide inhibits loop-type annealing more effectively than zipper-type annealing is shown in Figure 7, which portrays the observed ratio of rates for zipper versus loop annealing as a function of argininamide concentration.

TAR DNA Structure. The effect of argininamide on NC's destabilization activity was investigated by recording the ensemble E_A histogram for immobilized double-labeled D/A-TAR DNA in the absence and presence of NC and argininamide. (These data were recorded without a complementary oligonucleotide present, since the goal here is to measure the intermolecular distribution of 3'/5' distances for TAR DNA, rather than the annealing kinetics.) As previously demonstrated, and reproduced in Figure 8 (top left), D/A-TAR DNA in the absence of NC exists exclusively in its relatively rigid closed "C" form.¹¹ The "C" form, which has the maximum number of possible Watson–Crick base pairing for this hairpin, is characterized by $\langle E_A \rangle$ values of 0.95–0.96 (indicating a relatively short 3'/5' distance) and a negligibly small autocorrelation amplitude (indicating only small amplitude 3'/5' excursions).¹⁴ The presence of argininamide has, as expected, no effect on the "C" form (Figure 8, top right) since binding with this ligand

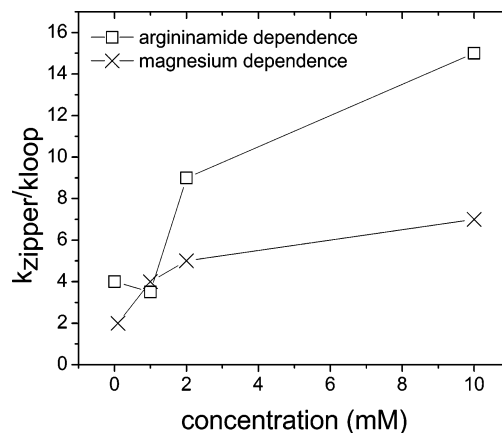


Figure 7. Comparison of the argininamide and magnesium dependence of the relative reaction rates for zipper vs loop annealing is shown. The relative rates at 10 mM argininamide were calculated from the respective peak areas of the products vs reactants. The lines are included as a guide only.

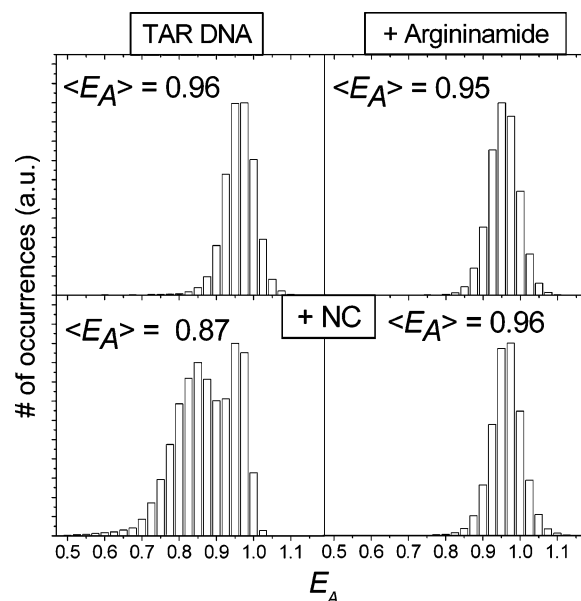


Figure 8. (Left) E_A histograms (binning time = 10 ms) for D/A-TAR DNA in buffer alone (top) and in the presence of 440 nM NC (bottom) are shown at 2 mM Mg^{2+} . (Right) The results for the same experimental conditions as in the left-hand panels, but in the presence of 10 mM argininamide, are compared.

tends to increase the strength of Watson–Crick base pairing, thus favoring the "C" form.

As shown previously, when D/A-TAR DNA is in the presence of NC at concentrations greater than 100 nM, the secondary structure in the region near the two bulges at the top of the stem is disrupted, resulting in a partial population of the "Y" form¹¹ and a resultant shift of $\langle E_A \rangle$ to 0.86. The "Y" form is manifested in the E_A histogram as an additional peak at lower E_A than the peak assigned to C (Figure 8, bottom left). A second manifestation of NC-induced partial melting is a large increase in the amplitude of the E_A autocorrelation amplitude, reflecting NC-induced DNA secondary structure fluctuations, as described in previous studies.^{11,14}

The suppression of NC activity on TAR DNA secondary structure by argininamide varies from no suppression at sub-millimolar concentrations to nearly complete suppression at 10

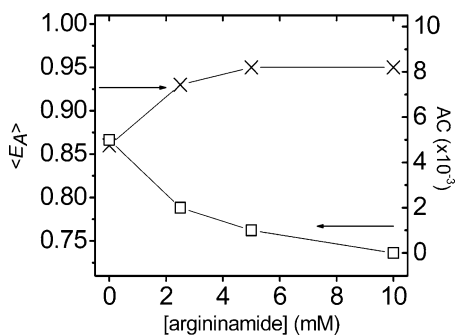


Figure 9. (Left) Average E_A for D/A-TAR DNA in the presence of 440 nM NC and various concentrations of argininamide are compared. (Right) The trend in average E_A AC at each concentration is shown.

nM argininamide (Figure 8, bottom right). For example, $\langle E_A \rangle$ of D/A-TAR DNA in the presence of NC and argininamide concentrations ranging from 0.2 to 10 mM were acquired at 2 mM Mg^{2+} (Figure 9). These results indicate that at low argininamide concentration (e.g., 0.2 mM), the effects on NC's ability to destabilize the secondary structure are negligible. Above 2 mM argininamide the E_A analysis shows that the average TAR DNA secondary structure is primarily in the "C" form. E_A autocorrelation analysis, however, reveals that secondary structure fluctuations are still measurable at all but the highest argininamide concentration (Figure 9). Interestingly, whereas the E_A autocorrelation amplitude decreased with addition of argininamide, the E_A autocorrelation lifetime remained constant (data not shown), indicating that although the argininamide induces an overall shift in the equilibrium away from the "Y" form of TAR DNA, when the hairpin occupies this state it exhibits the same complex dynamics reported in earlier studies to be important for annealing to occur.^{11,14}

A Mechanistic Interpretation of the Kinetic Inhibitory Effect of Argininamide. We have previously hypothesized that the NC-induced formation of the Y secondary structure of TAR DNA provides a low activation energy pathway for annealing of TAR DNA with oligonucleotides. The correlation observed herein between effects of added argininamide on the equilibrium population (concentration) of the "Y" form and the annealing rates of TAR DNA with oligonucleotides is highly consistent with this hypothesis. Qualitatively, these effects can be understood in terms of the model in Figure 1. The addition of argininamide apparently increases the relative stability of duplex secondary structures, i.e., those with greater Watson–Crick base pairing, thereby reducing the relative population of the partially melted oligonucleotides, e.g., "Y", which are key intermediates in the annealing mechanism.

Binding between DNA hairpins and arginine (an analogous ligand to argininamide) has been previously observed, although shown to be weaker than binding to the analogous RNA hairpin.²³ Other studies suggest that DNA/argininamide binding occurs through an alternate mechanism (i.e., through minor groove hydrogen-bonding interactions with base edges rather than with phosphate groups).²⁴ The distribution of binding sites on TAR DNA in the annealing reaction is not well established, but must be extremely complex, since partly melted TAR DNA presents multiple thermally accessible secondary structures with different degrees of melting of the four internal bulges.¹¹ We hypothesize that the observed preferential inhibition of loop

annealing may be due to a selective stabilization of this region by argininamide, although there is no direct evidence for this proposal.

It is important to note that the general effects of argininamide on the equilibrium structure of TAR DNA and on the annealing rate are analogous to those reported previously by us^{4,11} for Mg^{2+} , namely, that they both decrease NC-induced TAR DNA fluctuations and slow down annealing kinetics with varying degrees of efficiency. Additionally, as shown in Figure 9, increased Mg^{2+} concentrations preferentially suppress loop-type annealing in a parallel fashion to argininamide. Furthermore, both argininamide and Mg^{2+} have been shown by others to decrease fluctuations in the TAR RNA hairpin.^{17,28} The various effects of Mg^{2+} may reflect both nonspecific charge interactions as well as specific binding interactions such as those reported previously for Mg^{2+} binding to the hairpin loop region of TAR RNA.²⁹ There does not exist, to our knowledge, similar structural characterizations by techniques such as NMR or X-ray analysis for the specific binding of Mg^{2+} or argininamide to the TAR DNA hairpin. Such analysis would be helpful to supplement what we have learned about the dynamics of strand transfer, namely, that both ions exhibit an enhanced inhibitory effect for annealing that involves the hairpin loop region.

However, both charge shielding and specific binding effects have been observed for Mg^{2+} , e.g., complex Mg^{2+} -dependent conformational changes were observed in an immobilized RNA three-way junction.³⁰ Thus, it is likely that both specific and nonspecific outer-sphere charge shielding by Mg^{2+} and argininamide play a role in the annealing reaction, i.e., by suppressing the binding of NC to TAR DNA. NC is known to favor binding to single-stranded nucleic acids, which increases the thermodynamic stability of partially melted structures like "Y".^{11,14} A decrease in the binding constant of NC to single-stranded regions due to charge shielding would decrease the annealing rate and the secondary structure fluctuation of TAR DNA.

Conclusions

SMFRET was used to examine how argininamide, a model inhibitor for HIV-1 functionality, modulates the chaperone activity of the NC in the minus-strand transfer step of HIV-1 reverse transcription, in vitro. Argininamide is observed to measurably inhibit the rate of NC-chaperoned annealing of TAR DNA with targeted oligonucleotides. The studies reveal that the argininamide inhibitory mechanism involves a shift of the secondary structure of TAR, away from the NC-induced partially melted "Y" form and toward the NC free "C" form. It was also found that the NC-induced nucleation of annealing of TAR is more effectively inhibited at the hairpin loop region rather than the terminal stem region, suggesting molecular-level interactions of argininamide and NC binding to key annealing intermediates.

Acknowledgment. We thank Drs. George Barany and Daniel G. Mullen and Ms. Brandie Kovaleski (all from University of

- (28) Al-Hashimi, H. M.; Pitt, S. W.; Majumdar, A.; Xu, W.; Patel, D. J. *J. Mol. Biol.* **2003**, *329*, 867.
 (29) Olejniczak, M.; Gdaniec, Z.; Fischer, A.; Grabarkiewicz, T.; Bielecki, L.; Adamiak, R. W. *Nucleic Acids Res.* **2002**, *30*, 4241.
 (30) Kim, H. D.; Nienhaus, G. U.; Ha, T.; Orr, J. W.; Williamson, J. R.; Chu, S. *Proc. Natl. Acad. Sci. U.S.A.* **2002**, *99*, 4284.

Minnesota, Minneapolis) for chemical synthesis of NC. The authors also thank Dr. I. Tinoco for helpful discussion and the reviewers for useful suggestions. This work was supported by NIH Grant GM65818 (P.F.B.), NIH Grant GM065056 (K.M.-F.), NIH postdoctoral National Research Service Award GM073534 (C.F.L.), and the Welch Foundation (P.F.B.).

Supporting Information Available: Derivation of E_A profile and parameters used for simulation and further data on the Mg^{2+} vs argininamide dependence of the annealing rates. This material is available free of charge via the Internet at <http://pubs.acs.org>.

JA071491R